

# Numerical models of faulting at oblique spreading centers

G. W. Tuckwell,<sup>1</sup> J. M. Bull, and D. J. Sanderson

Department of Geology, University of Southampton, Southampton Oceanography Centre  
Southampton, England, United Kingdom

**Abstract.** Obliquely spreading mid-ocean ridges, such as the Reykjanes Ridge, display two distinct fault sets distinguishable by orientation and position: on-axis faults are oriented oblique to both the trend of the axis and the normal to the relative plate separation vector, while faults on the flanks strike approximately parallel to the ridge axis. Numerical modeling techniques are used here to simulate the development of faulting on the Reykjanes Ridge. Stresses acting in a cross section through the lithosphere at a slow spreading ridge are investigated using the fast Lagrangian analysis of continua (FLAC) explicit difference modeling software. The predicted stresses from the cross-sectional models are imposed as a condition in boundary element models of fracture propagation and linkage. On-axis fault simulations run under conditions similar to the Reykjanes Ridge successfully reproduce the mapped distribution of faults and predict the observed orientation of the axial volcanic ridges. Simulations of fractures away from the axis show the development of axis-parallel faults by the interaction and linkage of fractures which have been rafted off-axis, also in accord with observations. Stresses modeled in cross section favor downdip displacement on faults dipping toward the ridge axis.

## 1. Introduction

The controls on the formation and evolution of faulting patterns observed at obliquely spreading centres, such as the Reykjanes Ridge, are poorly understood. The Reykjanes Ridge is located immediately south of Iceland, extending from 56°30'N to 63°30'N, and is the longest section of obliquely spreading ridge in the world's oceans today (Figure 1). The ridge is continuous with no transform offsets [Talwani *et al.*, 1971; Johnson *et al.*, 1971; Jackoby, 1980; Appelgate and Shor, 1994] and is oriented N036°E. The Reykjanes Ridge spreads obliquely with the relative plate separation vector oriented at 099°, at a half rate of 10 mm yr<sup>-1</sup> (DeMets *et al.*, 1990).

Two distinct fault sets are present, distinguishable by orientation and position [Murton and Parson, 1993; McAllister *et al.*, 1995] (Figure 2). On-axis faults strike at 022° (i.e. 14° oblique to the trend of the ridge axis and 13° oblique to the normal to the relative plate separation vector) [Appelgate and Shor, 1994; Tuckwell *et al.*, 1996]. Axial volcanic ridges (AVRs), volcanic constructs associated with the emplacement of new material at the axis, are arranged in echelon along the axis with orientations similar to the on-axis faults [Appelgate and Shor, 1994]. Off-axis faults strike at a low angle to the ridge, with an average strike of 029° (i.e. 7° oblique to the ridge trend) and predominantly dip toward the ridge axis [McAllister *et al.*, 1995]. This preferred dip direction has been observed at all slow and intermediate spreading ridges [Carbotte and Macdonald, 1990]. The orientation of off-axis fractures implies a rotation of driving stress with distance from the spreading axis [Murton and Parson, 1993; McAllister *et al.*, 1995]. This study addresses the nature of the stresses acting both on- and off-axis and

investigates the development and evolution of fracture systems formed in these regimes.

For simplicity we treat on- and off-axis fractures separately. On-axis fractures are taken as those which form in the neovolcanic zone (Figure 3). This is the area in the center of the spreading axis where active volcanism occurs and has an average width of 12 km on the Reykjanes Ridge [McAllister *et al.*, 1995]. Off-axis fractures are those which bound the neovolcanic zone on either side of the axis. Our model assumes that the neovolcanic zone is roughly equivalent to a mechanically weak zone represented by a thin brittle lid overlying a weak zone which acts as a conduit for rising mantle material between the diverging lithosphere plates. Either side of this weak zone, the lithosphere cools with distance from the axis, thus becoming mechanically stronger with thickening of the brittle layer (Figure 3).

Two numerical modeling approaches have been used to investigate the nature of the stresses acting on the flanks of the axis and to simulate the development of a system of fractures in a given stress regime. Boundary element modeling code has been written using the displacement discontinuity method of Crouch and Starfield [1990] to simulate the propagation and linkage of a large number of fractures in a two-dimensional infinite elastic medium. The stress field operating off-axis is investigated by the construction of a model through a cross section of lithosphere using the Fast Lagrangian Analysis of Continua (FLAC) explicit difference software [ITASCA Consulting Group Inc., 1993]. FLAC is a two-dimensional explicit difference code based upon a Lagrangian calculation scheme [Cundall and Board, 1988; Coetzee *et al.*, 1995]. FLAC has several built-in constitutive models which permit the simulation of highly nonlinear response representative of geologic materials [e.g. Cundall, 1990].

## 2. Boundary Element Model

The boundary element modeling approach has been widely used in previous studies of fracture development and interaction [e.g. Sempere and Macdonald, 1986; Olsen and Pollard, 1991; Renshaw and Pollard, 1994; Renshaw and Harvey, 1994]. In the model,

<sup>1</sup>Now at Department of Earth Science, University of Liverpool, Liverpool, England, United Kingdom.

Copyright 1998 by the American Geophysical Union.

Paper number 97JB03673.  
0148-0227/98/97JB-03673\$09.00

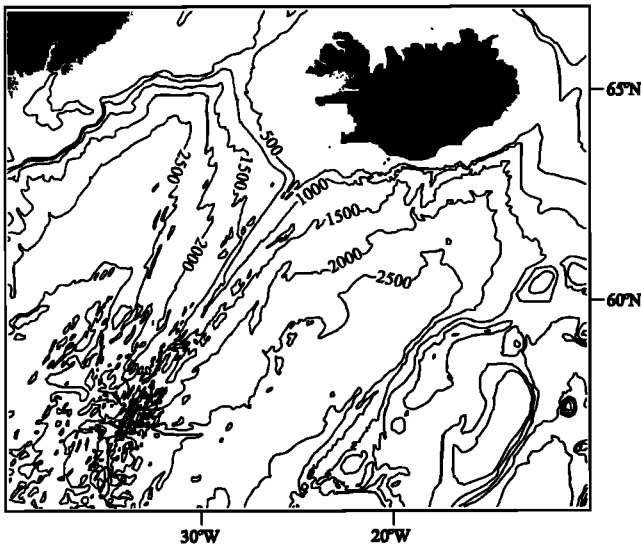


Figure 1. Bathymetric chart of the Reykjanes Ridge south of Iceland showing the isobaths in meters.

the fractures develops iteratively by three processes: propagation, tip-to-tip linkage and tip-to-wall linkage. The stress field is recalculated after each growth event.

Propagation is simulated by adding a new element to the tip of the crack, thus increasing its length. The direction of propagation (i.e. the orientation of the new element) is calculated from the stresses acting on the crack tip using the maximum circumferential stress theory [Erdogan and Sih, 1963]. This theory states that propagation should occur in the direction which maximizes circumferential tension near the crack tip and in which the resolved shear stress is zero (Figure 4). Propagation will occur in the direction,  $\theta$ , defined by

$$K_I \sin\theta + K_{II} (3 \cos\theta - 1) = 0, \tag{1}$$

where  $K_I$  and  $K_{II}$  are the mode I and mode II stress intensity factors, respectively, and  $\theta$  is measured clockwise from the crack tip. Propagation will occur if the stress intensity at the crack tip,  $K_{ip}$ , is greater than the fracture toughness of the material,  $K_{Ic}$  [Lawn and Wilshaw, 1975], where

$$K_{ip} = \cos\frac{\theta}{2} (K_I \cos^2\frac{\theta}{2} - \frac{3}{2} K_{II} \sin\theta). \tag{2}$$

each fracture is represented by a number of short linear sections termed elements (Figure 4). Each element represents a displacement discontinuity which deforms when a far-field stress field is applied, affecting the local stress field around it. Growth of

$K_{ip}$  is calculated for every fracture tip, and the maximum value for the model is found. The length of the new element added at a propagating fracture tip is proportional to  $(K_{ip} - K_{Ic})$ , with the value of  $K_{Ic}$  giving a length of zero and the maximum value of  $K_{ip}$  for the

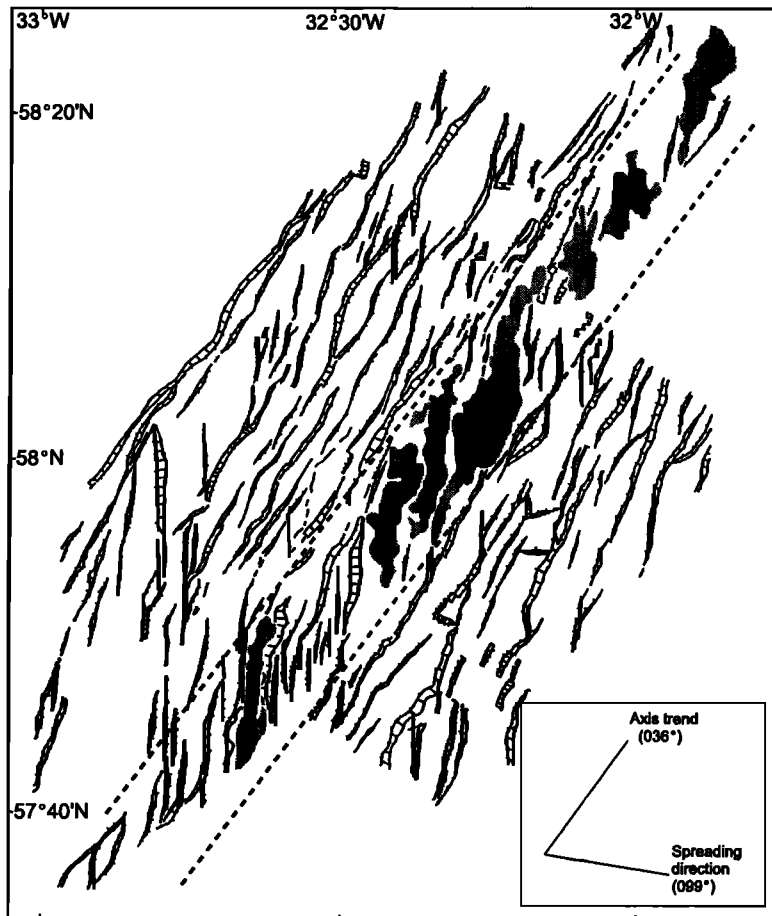


Figure 2. Structural map of the southern section of the Reykjanes Ridge. The shaded areas correspond to axial volcanic ridges (AVRs). Faults are shown by cross-hatched lines. Dashed lines delineate the near-axis weak zone where faults and AVRs are oblique to both the axis trend and the normal to the spreading vector. Outside this zone, faults are typically longer and oriented at a lower angle to the axis trend. Redrawn from Murton and Parson [1993], Copyright 1993, with permission from Elsevier Science.

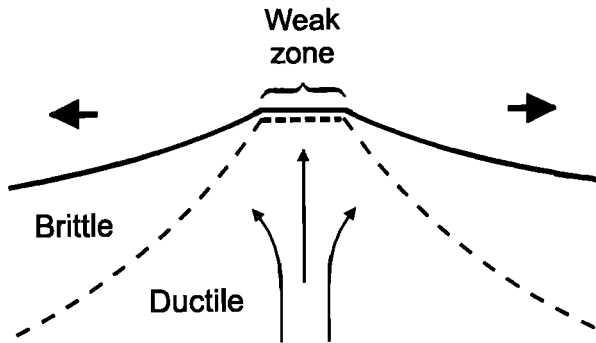


Figure 3. Schematic geometry and rheology of a cross section through a spreading ridge.

model giving the length specified in the model parameters as the maximum length for a new element. By this mechanism, fractures subjected to greater differential stress will increase in length more and hence propagate faster than others.

Fracture linkage occurs by the interaction of process zones ahead of a propagating fracture. The process zone may be defined as an extensively damaged area extending ahead of the fracture in the direction of propagation [Freidman *et al.*, 1972; Segall and Pollard, 1983; Simpson, 1983; Cox and Scholz, 1988; Bjarnason *et al.*, 1992; Cowie and Scholz, 1992]. The length of the process zone extending ahead of a propagating fracture is assumed to be proportional to  $K_{tip}$ , with the maximum value taken as 10% of the fracture length [An and Sammis, 1996]. Tip-to-tip linkage will occur if the process zones of two propagating fractures overlap (Figure 5a). Tip-to-wall linkage will occur if the process zone of a propagating fracture encounters the wall of another fracture (Figure 5b).

### 3. Near-Axis Faults

Fractures on the axis of the Reykjanes Ridge are oblique to both the trend of the axis and the normal to the relative plate separation vector [Appelgate and Shor, 1994; Tuckwell *et al.*, 1996] and have the same orientation as the AVR's (Figure 2). Deformation at oblique spreading centers may be considered in terms of a

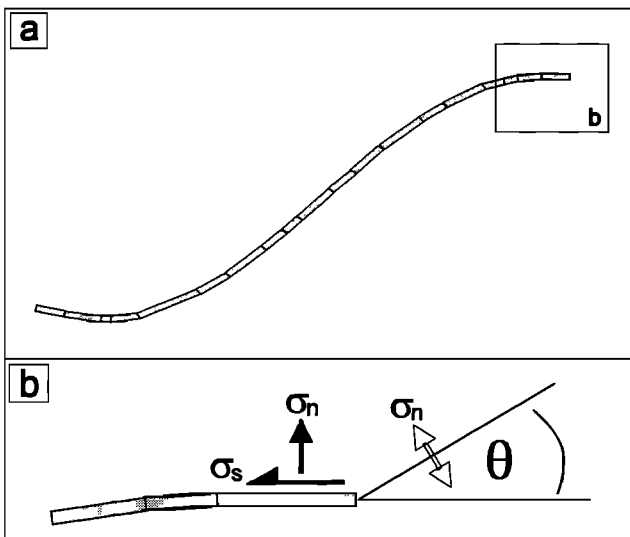


Figure 4. (a) Representation of a curved crack by a number of short linear boundary elements. (b) Fractures propagate at an angle  $\theta$  along a path of zero resolved shear stress.

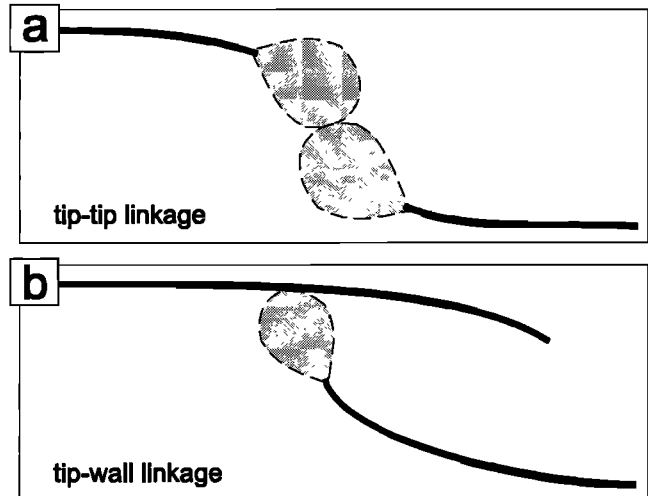
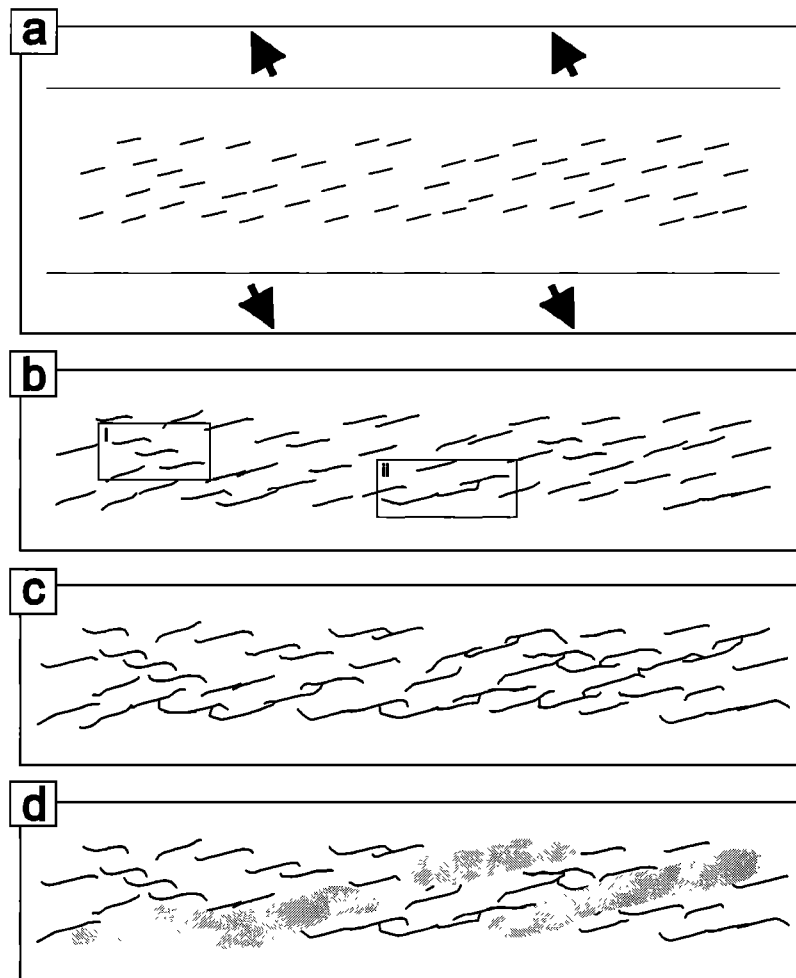


Figure 5. Interaction of process zones ahead of propagating fractures.

displacement vector with a component of opening normal to the ridge axis and a component of shear along it. The transtension model of Sanderson and Marchini [1984] relates the orientation of principal stresses to the displacement vector. A simple geometrical relationship exists between the displacement vector and the orientation of the principal compressive stress [McCoss, 1986] and thus also the orientation of extensional fractures. Tuckwell *et al.* [1996] demonstrated that fractures observed at oblique spreading centres form in response to a transtensional stress field produced by plate separation. They also hypothesised that larger on-axis fractures are exploited by volcanism to form AVR's, explaining the identical distribution of orientations.

The boundary element model was used to simulate the development of a system of fractures within the near-axis weak zone of the Reykjanes Ridge. The parameters used are listed in Table 1. The magnitude of stress acting at the axis of a spreading ridge is poorly constrained. Numerical models of upwelling material in a vertical conduit estimate ridge strength to be of the order of 10-30 MPa [Lachnbruch, 1973] and is expected to vary with spreading rate. For our model the magnitude of the stress acting at the axis is taken as 30 MPa and is oriented such that the principal compressive stress is at an angle of  $14^\circ$  to the trend of the ridge axis, as calculated from transtension theory. Fifty fractures were initiated at random positions within an elongate area representing a short section of ridge (Figure 6a). Newly initiated fractures are oriented perpendicular to the minimum horizontal compressional stress  $S_h$  and are sufficiently short so as not to significantly influence the regional stress field. As the model is run and the fractures grow, mechanical interaction occurs as the propagation path of one fracture is influenced by the perturbation in the local stress field around another, causing the propagation paths of fracture tips to curve in toward neighboring fractures (Figure 6b). The processes of tip-to-tip and tip-to-wall linkage may be seen to occur as fracture tips near neighboring fractures (Figure 6b). If the model is run further, the pattern generated comprises fractures with a wide range of lengths with orientations distributed about an angle of  $14^\circ$  to the trend of the ridge, the expected orientation of fractures in this transtensional stress field (Figure 6c). Linkage has produced a small number of longer fractures arranged en echelon along the axis. If the longer fractures are exploited by volcanism to form AVR's, as hypothesised by Tuckwell *et al.* [1996], then a realistic morphological picture of the Reykjanes Ridge near-axis region is produced (Figure 6d), which can be compared directly with the structural map in Figure 2.



**Figure 6.** Boundary element model of the development of a system of fractures formed on-axis. (a) Fifty fractures are initiated in a transtensional stress field. Arrows represent the displacement on the boundaries of the zone of deformation. (b) As the model is run fractures interact (i) and link (ii). (c) The final distribution of fractures is shown. (d) Predicted axis morphology is shown if longer fractures are exploited by volcanism to produce axial volcanic ridges (AVRs), shown as shaded areas.

#### 4. Off-Axis Faults

In contrast to on-axis faults at oblique spreading centers, off-axis faults are oriented at a low angle to the axis trend (Figure 2). Off-axis faults typically extend to greater lengths and have greater displacements than on-axis faults [McAllister *et al.*, 1995]. Faults observed on the flanks of the Reykjanes Ridge are characterized by their irregular shape and branching structures where the trace of one fault splits into two or more splays (Figure 2).

The stresses acting in a cross section through the lithosphere of a slow spreading ridge were modeled using the FLAC two-dimensional explicit difference software and parameters appropriate to the Reykjanes Ridge (Table 1). The model extends to a horizontal distance of 400 km from the ridge axis and a depth of 70 km, with the finest grid mesh at the axis (Figure 7). A simple plate cooling model, with bathymetry proportional to the square root of lithosphere age is used to model the geometry and temperature of the lithosphere [Parsons and Sclater, 1977]. A rheological profile is determined by calculating the brittle and ductile strengths of the material. The deformation process is taken to be that which operates at the lowest stress.

Brittle strength is calculated using a frictional slip criterion in which the lithosphere is assumed everywhere to be fractured such

that in any given stress field failure may occur by frictional slip along a preexisting fracture (Byerlee's law). Thus the brittle strength of a material can be written in terms of stress difference, overburden pressure, and pore fluid pressure as [Kirby, 1983]

$$\sigma_1 - \sigma_3 \geq \beta \rho g z (1 - \lambda), \quad (3)$$

where  $\sigma_1$  and  $\sigma_3$  are the maximum and minimum compressive stresses respectively,  $\rho$  is the density of the material,  $g$  is the acceleration due to gravity,  $z$  is the depth,  $\lambda$  is the ratio of pore fluid pressure to overburden pressure, and  $\beta$  is a parameter depending on the type of faulting, with values of 3, 1.2, and 0.75, for thrust, strike-slip, and normal faulting respectively [Ranalli and Murphy, 1987]. The friction along a fracture plane is largely independent of lithology, even for materials such as quartz and calcite with widely differing strengths. At high confining pressures it has been shown experimentally that the stress required to form a fault exceeds the stress required to cause sliding on an optimally oriented fault [Byerlee, 1978]. Thus at any depth the brittle strength may be taken as the differential stress required to produce slip on a preexisting fracture.

The brittle strength is therefore largely stress dependent and may be considered to be unaffected by temperature. This relationship

**Table 1.** Parameters Used in Numerical Models

Property	Value	Reference
Fracture toughness	1.9 Mpa m <sup>1/2</sup>	<i>Jones et al.</i> [1996]
Poissons ratio	0.43	<i>Wright et al.</i> [1995]
Shear modulus	3400 MPa	<i>Wright et al.</i> [1995]
Density (crust, mantle)	2900, 3300 kg m <sup>-3</sup>	<i>Shaw and Lin</i> [1996]
Power law creep		<i>Ranalli and Murphy</i> [1987]
<i>A</i> (crust, mantle)	8x10 <sup>25</sup> , 4x10 <sup>12</sup> Pa <sup>-n</sup> s <sup>-1</sup>	
<i>n</i> (crust, mantle)	3.4, 3.0	
<i>Q</i> (crust, mantle)	269,000, 540,000 J mol <sup>-1</sup>	
Thermal diffusivity	10 <sup>-6</sup> m <sup>2</sup> s <sup>-1</sup>	<i>Parsons and McKenzie</i> [1978]
Coefficient of thermal expansion	3x10 <sup>-5</sup>	<i>Kirby</i> [1983]
Reykjanes Ridge		
Crustal thickness	8 km	<i>Searle and Laughton</i> [1981]
Half spreading rate	10 mm yr <sup>-1</sup>	<i>De Mets et al.</i> [1990]

has been confirmed experimentally predicting a limiting stress difference for frictional sliding along thrust, strike-slip and normal faults. However, at low differential stress (up to 50 MPa) the variability in the value of friction is large, and few data are available for normal stress levels up to 1000 MPa. Most data are for normal

stress levels of up to 250 MPa, corresponding to a depth of approximately 20 km, within which range the value for frictional strength may vary by a factor of 2 [*Brodie*, 1991]. For the purposes of the model an average crustal density,  $\rho$ , is taken to be  $2.9 \times 10^3$  kg m<sup>-3</sup>. Assuming hydrostatic pore fluid pressure,  $\lambda=0.36$  at all depths.

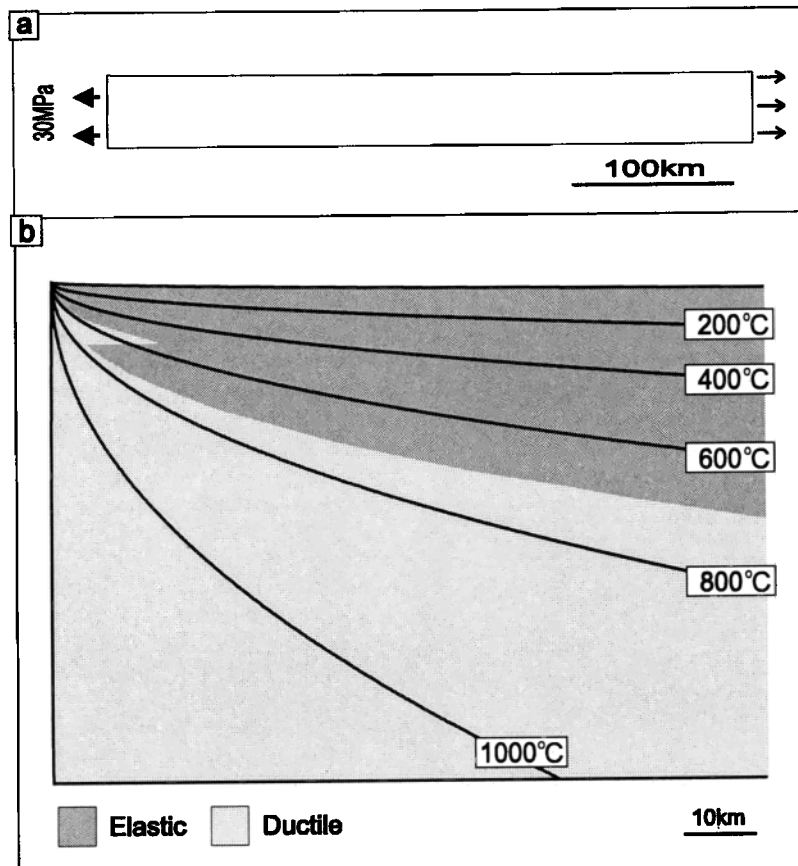


**Figure 7.** Explicit difference model of a cross section through the lithosphere at a slow spreading ridge. (a) The model extends to a depth of 70 km and to a distance of 400 km off axis. The axis is held with a resistive stress of 30 MPa, and the right-hand edge of the model is pulled at a constant velocity. (b) Thermal and rheological profile near the axis of a slow spreading ridge.

Strength values predicted by frictional failure are likely to be upper limits since the fault plane may be lubricated with clay minerals with a lower coefficient of friction [Ranalli and Murphy, 1987].

Ductile strength may be defined as the differential stress required to plastically deform the material at a specified strain rate. Ductile deformation may occur by three mechanisms: cataclasis, intracrystalline plasticity, and diffusive mass transfer. All these processes occur on the microscopic scale. For strain rates and temperatures prevalent in the lithosphere, dislocation creep is generally assumed to be the dominant mechanism [Kirby, 1983]. On a macroscopic scale the plastic deformation of materials may be calculated by a power law-creep relationship. For a given chemical environment the steady state creep rate  $\dot{\epsilon}_s$  is influenced by temperature  $T$  and differential stress  $\sigma$ , via the Dorn [1956] equation

$$\dot{\epsilon}_s = A \sigma^n \exp\left(\frac{-Q}{RT}\right), \quad (4)$$

where  $R$  is the gas constant,  $A$ ,  $n$  and  $Q$  are experimentally determined material parameters which are approximately stress and temperature independent. The material parameter  $n$  is termed the stress exponent and is dimensionless, the parameter  $Q$  is the creep activation energy of the material and has units  $\text{J mol}^{-1}$ , parameter  $A$  has units  $\text{Pa}^{-n} \text{s}^{-1}$ . We assume a diabase rheology for the crust and a dry olivine rheology for the mantle [Chen and Morgan, 1990; Shaw and Lin, 1996]. Material parameters are listed in Table 1. Crustal thickness is assumed to be 8 km [Searle and Laughon, 1981]. Results from models run with crustal thicknesses of 6 km and 10 km do not vary significantly from those presented here.

A two-dimensional rheological profile through a cross section of oceanic lithosphere may thus be constructed (Figure 7). The brittle layer is modeled as elastic, rather than brittle to investigate the stresses that drive the deformation of the brittle lithosphere. Allowing the brittle layer to fail would relieve these stresses. Ductile material is modelled using the WIPP power law creep criteria, a constituent model in the FLAC software which provides a solution to (4) [ITASCA Consulting Group Inc., 1993]. Gravitational forces applied at each node of the explicit difference grid  $F_g$  are calculated by

$$F_g = gV\rho_0(1-\alpha T), \quad (5)$$

where  $g$  is the acceleration due to gravity,  $V$  is the volume of material represented by the node,  $\rho_0$  is the density of material at  $0^\circ\text{C}$ ,  $\alpha$  is the coefficient of thermal expansion, and  $T$  is the temperature. A resistance to plate separation at the ridge axis of 30

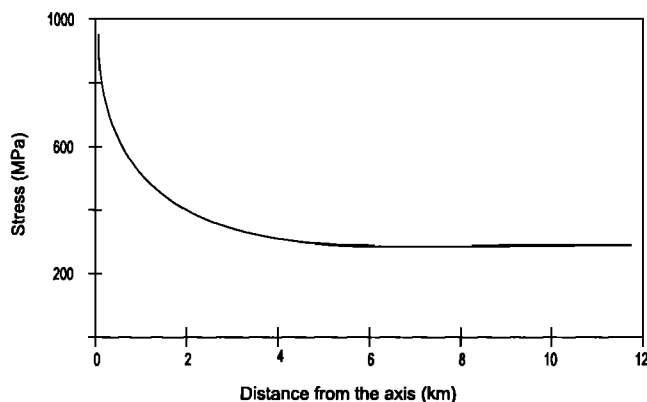


Figure 8. Graph of horizontal stress in the brittle layer versus distance from the ridge axis.

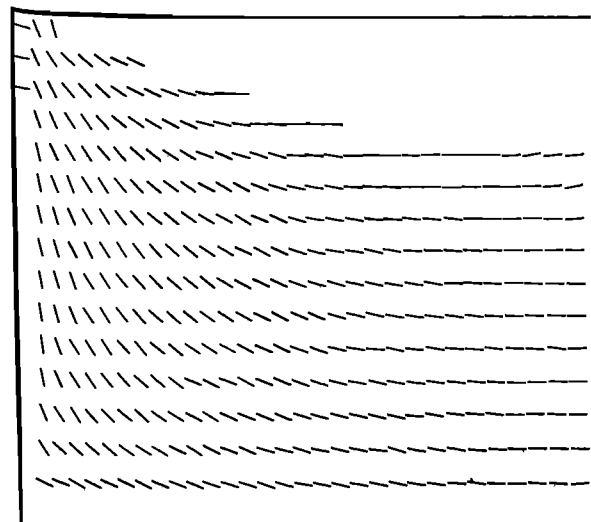


Figure 9. The orientation of principal stress axes in a cross section through the lithosphere at a slow spreading ridge.

MPa is assumed [Lachenbruch, 1973] and a velocity is applied to the right-hand edge (Figure 6a).

If horizontal stress were developed solely due to the resistance to plate separation at the axis, then the magnitude of horizontal stress would not be expected to exceed the magnitude of this resistance. The magnitude of horizontal stress decreases from approximately 1000 MPa near to the axis to 300 MPa at a distance of 6 km (Figure 8). This stress is generated by the gravitational forces acting on the brittle lithosphere as its density increases off-axis, the near-ridge effect of the ridge-push force and is an order of magnitude higher than that which can be supported at the ridge axis. Thus on the flanks of the ridge it may be assumed that stresses are acting almost normal to the trend of the ridge. It is clear that such large extensional stresses could not be supported by the lithosphere, which would fail and deform. It is important to emphasize, however, that the off-axis stress field is dominated by these large stresses and that this deformation would be driven by ridge normal extension. In cross section the principal extensional stress axes are inclined away from the ridge axis (Figure 9), favoring downdip displacement on faults dipping toward the ridge axis.

The boundary element model was used to investigate the development of fractures on the flanks of the axis. Material properties are assumed to be homogeneous in the plane of the model. A system of faults formed on-axis, modeled as described previously, is assumed to have been rafted off-axis (Figure 10a). Longer fractures that formed on-axis are assumed to have been sealed when exploited by volcanism to form AVRs. This system of fractures is then allowed to develop in an extensional stress field oriented perpendicular to the ridge axis trend (Figure 10b). Fractures propagate and link to develop long, irregular structures oriented at a low angle to the trend of the ridge. The length weighted average orientation of fractures shown in Figure 10b is  $10 \pm 2^\circ$  to the trend of the ridge, at 95% confidence. Thus off-axis fractures develop at a lower angle to the ridge trend than those on axis. It is principally the process of fracture linkage driven by a stress field oriented orthogonal to the axis trend which acts to rotate the average strike of off-axis fractures toward axis parallel.

## 5. Off-Axis Morphology

The irregular nature of the fractures is a function of the orientation and length of the starting fractures. Studies by Bergman

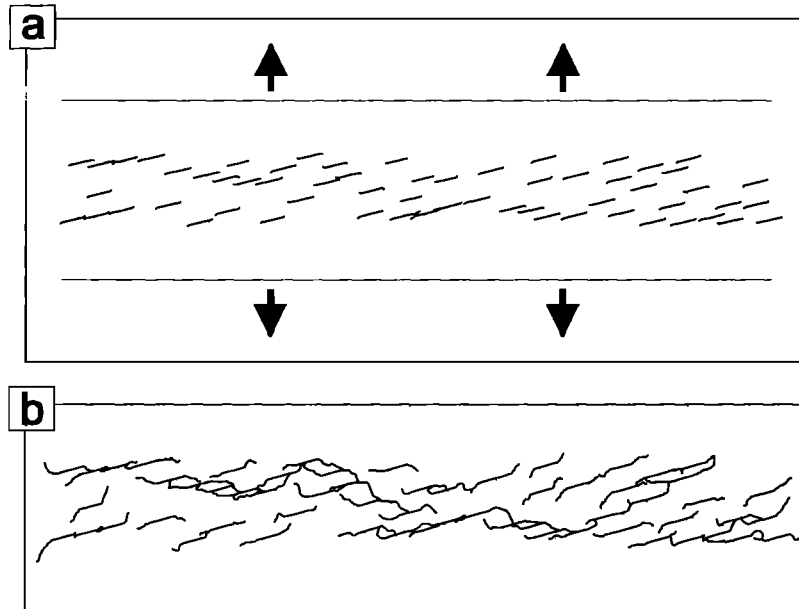


**Figure 10.** Boundary element model of the development of fractures off-axis. (a) A system of fractures formed on-axis is assumed to have been rafted off-axis and is subjected to a stress field oriented normal to the trend of the ridge axis. Arrows represent the displacement on the boundaries of the zone of deformation. (b) The process of fracture linkage produces long irregular fractures oriented at a lower angle to the axis trend.

and Solomon [1990] and Shaw and Lin [1993] suggest that off-axis morphology at slow spreading ridges is the expression of rotated normal fault blocks. Consequently, off-axis morphology may offer an insight into the nature of fractures which have been rafted off-axis. Three boundary element models of off-axis fracture development have been run with the same initial distribution of

fractures but with different far-field stress histories. In an extensional stress field, fractures link to produce long, relatively straight structures (Figure 11a). Fractures grown in an extensional stress field from a system of fractures formed in a transtensional stress field produce more irregular fractures than those in the previous example (Figure 11b). A system of fractures formed in a

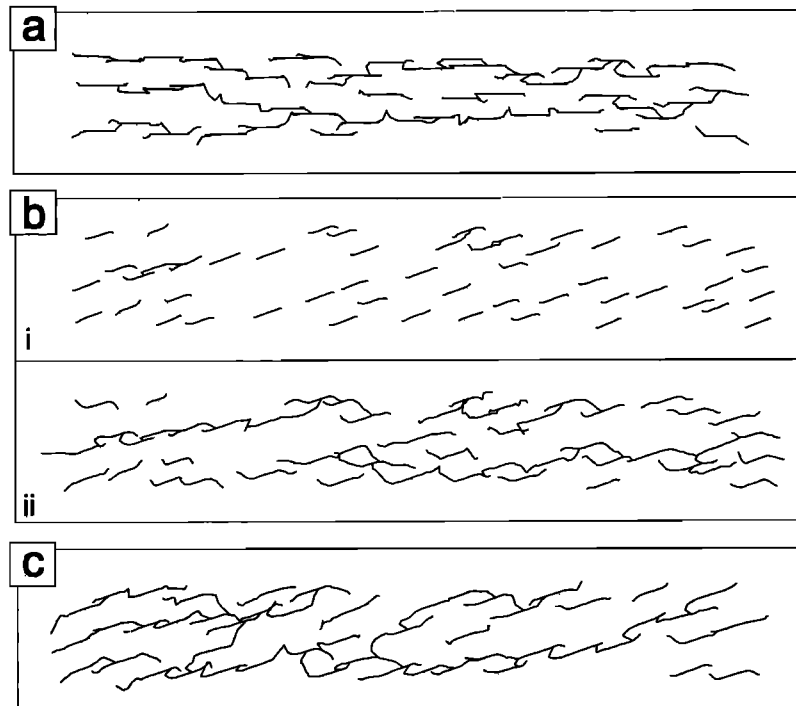


**Figure 11.** Comparison of three models run with the same starting distribution of fractures but with different far-field stress histories. (a) Fractures grown entirely in pure extension. (b) Fractures initially formed in a transtensional stress field (i), grown in an extensional stress field (ii). (c) Fractures grown entirely in a transtensional stress field

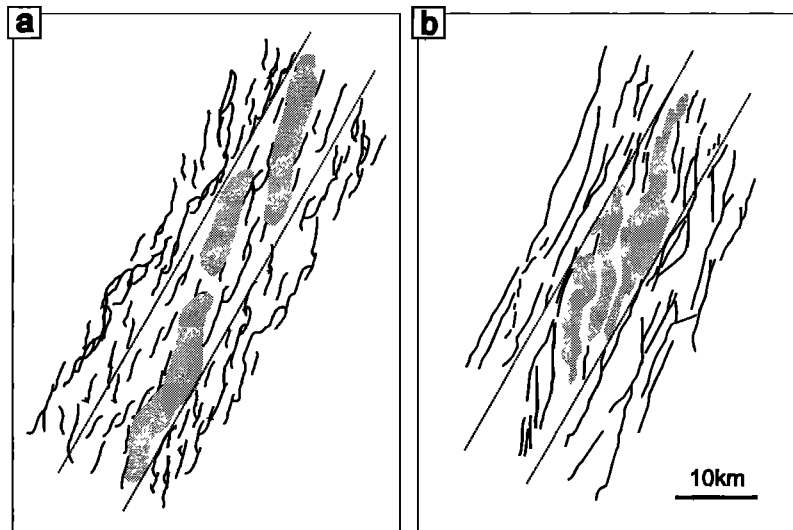


**Figure 12.** (a) Diagram of a section of obliquely spreading ridge constructed from models of on- and off-axis faulting. Shaded areas represent axial volcanic ridges (AVRs). (b) Fault map of the southern Reykjanes Ridge about 58°N. Redrawn from *Murton and Parson* [1993]. For both plots, dashed lines delineate the “near-axis” zone.

transensional stress field produces very irregular structures (Figure 11c). Our model predicts a more irregular off-axis morphology at oblique spreading ridges. The effect of spreading obliquity on the ridge morphology may be exaggerated by longer fractures being rafted off-axis. If volcanism exploits the longest fractures at the axis, as these are expected to be deepest [Cowie and Scholz, 1992; Wright *et al.*, 1995], then an increase in volcanic activity may exploit a greater number of on-axis fractures, reducing the average length of fractures which are rafted off-axis. Thus off-axis morphology may be influenced by past spreading obliquity and magmatic activity. The application of this modeling approach to the development of ridge morphology is the subject of further study.

## 6. Comparison With Reykjanes Ridge

A model of on-axis fractures may be positioned between two off-axis fracture models to approximate a complete fault map for a short section of ridge (Figure 12a). This may be directly compared with

a fault map of a section of the Reykjanes Ridge at approximately 58°N, produced from interpretation of SeaMARC II backscatter data [Murton and Parson, 1993] (Figure 12b). Here we use the *Tuckwell et al.* [1996] hypothesis that AVRs exploit the longer near-axis fractures. Both maps clearly show the on-axis faults and AVRs oriented oblique to both the trend of the axis and the normal to the spreading direction and distributed about an angle of approximately 14° to the trend of the ridge axis. Off-axis faults are oriented approximately axis-parallel and are irregular in shape showing branching in the trace of the fault, consistent with structures formed in the model by the process of tip-to-wall linkage.

The distribution of fault length versus azimuth plotted from the data [Appelgate and Shor, 1994] is very similar to that from the model (Figure 13). Data measured from the model were taken from the orientation of each boundary element, weighted by the element length. Values of fault length at discrete fracture trends from the data and the model agree well, with a correlation coefficient of 0.95, indicating that the stress regimes used as a boundary condition for

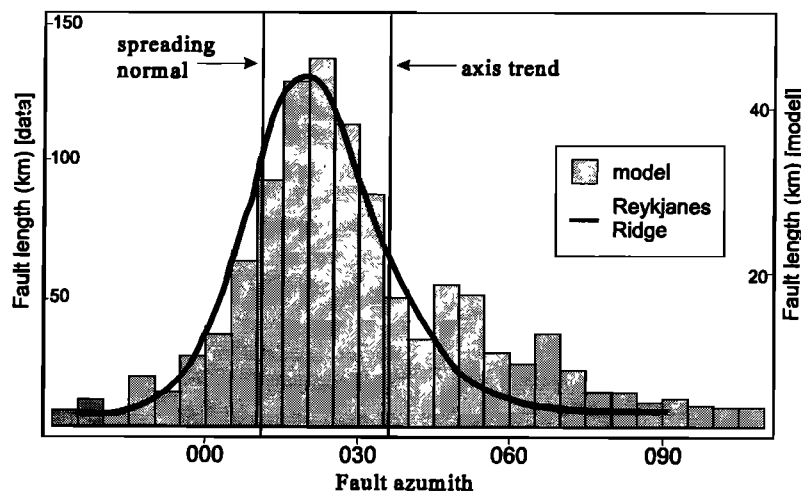


**Figure 13.** Histograms of fault length against azimuth. Blocks represent data taken from models of fracture propagation and linkage; the line represents fault data for the Reykjanes Ridge between 55°50'N and 63°00'N (redrawn from *Appelgate and Shor* [1994, Figure 9]). Refer to text for details.

the models of fracture propagation are capable of producing the structural features seen at the Reykjanes Ridge. Thus a slow spreading ridge may be modeled as having a weak zone centred at the axis, which at the surface deforms by brittle fracture in response to plate separation. This weak zone is bounded either side by relatively strong brittle lithosphere, which deforms in response to the large axis normal stresses generated by gravitational effects as its density increases off-axis.

## 7. Conclusions

Boundary element models of fracture propagation and linkage generate systems of fractures of varying length and with a distribution of orientations in agreement with that expected for a transtensional stress field. The process of linkage produces long fractures which may be exploited by volcanism to produce axial volcanic ridges (AVRs) and are arranged en echelon along the length of the ridge axis.

Extensional stress on the flanks of the ridge, modeled using the FLAC explicit difference modeling software, is an order of magnitude higher than that acting on-axis. This stress is gravity driven, generated by the variation of topography and density with distance from the ridge, and acts normal to the ridge trend. This is the near-ridge expression of the ridge push force. In cross section the orientations of principal extensional stress axes favor downdip displacement on faults dipping toward the axis.

Fractures observed on the flanks of the ridge may be modeled by assuming a distribution of fractures formed on-axis has been rafted off-axis, where fractures propagate in an extensional stress field oriented normal to the ridge trend. The length and obliquity of the rafted fractures control the irregularity of the off-axis faults and are expected to have a significant effect on off-axis morphology. Branches in the trace of fractures observed on the Reykjanes Ridge are produced in the model by the process of tip-to-wall linkage.

Combining models of on- and off-axis faults produces a realistic representation of the structure of an obliquely spreading ridge. Histograms of fault length against azimuth for the models and the real data are statistically similar, indicating that the fracture distribution produced by the model is close to that which exists on the Reykjanes Ridge. This implies that the stress regimes applied as a boundary condition in the models of fracture propagation and linkage are capable of producing the structural features seen at obliquely spreading ridges. Thus slow, obliquely spreading ridges may be modeled as having a weak central zone which deforms in response to plate separation, bounded on either side by relatively strong lithosphere with brittle thickness and strength increasing off-axis.

**Acknowledgments.** This work has benefited from discussions with L. M. Parson and B. J. Murton. G.W.T. is supported by a studentship from the Department of Geology, University of Southampton. This manuscript has been improved by careful reviews by J. Goff, G. Neumann, and an anonymous reviewer.

## References

- An, L.-J., and C. G. Sammis, A cellular automation for the development of crustal shear zones, *Tectonophysics*, 253, 247-270, 1996.
- Appelgate, B., and A. N. Shor, The northern Mid-Atlantic and Reykjanes Ridges: Spreading centre morphology between 55°50'N and 63°00'N, *J. Geophys. Res.*, 99, 17,935-17,956, 1994.
- Bergman, E. A., and S. C. Solomon, Earthquake swarms on the Mid-Atlantic Ridge: Products of magmatism or extensional tectonics?, *J. Geophys. Res.*, 95, 4943-4965, 1990.
- Bjarnson, I. T., P. Cowie, M. H. Anders, L. Seeber, and C. H. Scholz, The Iceland 1912 earthquake rupture: Growth and development of a nascent transform system, *Bull. Seismol. Soc. Am.*, 83, 415-435, 1992.
- Byerlee, J. D., Friction of rocks, *Pure Appl. Geophys.*, 116, 615-626, 1978.
- Carbotte, S. M., and K. C. Macdonald, Causes of variation in fault-facing direction on the ocean floor, *Geology*, 18, 749-752, 1990.
- Chen, Y., and W. J. Morgan, A non-linear rheology model for mid-ocean ridge axis topography, *J. Geophys. Res.*, 95, 17,583-17,604, 1990.
- Coetzee, M. J., R. D. Hart, P. M. Varona, and P. A. Cundall, *FLAC Basics*, ITASCA Consulting Group, Minn., 1995.
- Cowie, P. A., and C. H. Scholz, Physical explanation for the displacement-length relationship of faults using a post-yield fracture mechanics model, *J. Struct. Geol.*, 14, 1133-1148, 1992.
- Cox, S. J. D., and C. H. Scholz, On the formation and growth of faults: An experimental study, *J. Geophys. Res.*, 93, 3307-3320, 1988.
- Crouch, S. L., and A. M. Starfield, *Boundary Element Methods in Solid Mechanics*, 322pp., Unwin, Hyman, Boston, Mass., 1990.
- Cundall, P. A., Numerical modelling of jointed and faulted rock, in *Mechanics of Jointed and Faulted Rock*, edited by J. Rossmanith, pp. 11-18, A. A. Balkema, Brookfield, Vt., 1988.
- Cundall, P. A., and M. Board, A microcomputer program for modelling large strain plasticity problems, in *Numerical Methods in Geomechanics, Proceedings of the 6th International Conference on Numerical Methods in Geomechanics*, edited by C. Swoboda, pp. 2101-2108, A. A. Balkema, Brookfield, Vt., 1988.
- DeMets, C., R. G. Gordon, D. F. Argus, and S. Stein, Current plate motions, *Geophys. J. Int.*, 101, 425-478, 1990.
- Dorn, J. E., Some fundamental experiments on high temperature creep, in *Proceedings of National Physical Laboratory Symposium, Creep and Fracture of Metals at High Temperatures*, pp. 89-138, Her Majesty's Stationery Office, London, 1956.
- Erdogan, F., and G. C. Sih, On the crack extension in plates under plane loading and transverse shear, *Trans. Am. Soc. Mech. Eng.*, 85, 519-527, 1963.
- Freidman, M., J. Handin, and G. Alani, Fracture-surface energy of rocks, *Int. J. Rock Mech. Min. Sci.*, 9, 757-766, 1972.
- ITASCA Consulting Group Inc., *Fast Lagrangian Analysis of Continua*, version 3.2, Minneapolis, Minn., 1993.
- Jacoby, W. R., Morphology of the Reykjanes Ridge crest near 62°N, *J. Geophys. Res.*, 47, 81-85, 1980.
- Johnson, G. L., P. R. Vogt, and E. D. Schneider, Morphology of the northeastern Atlantic and Labrador Sea, *Ger. Hydrogr. J.*, 24, 49-73, 1971.
- Jones, C., P. G. Meredith, S. A. F. Murrell, and P. R. Sammonds, Mechanical properties of mid-ocean ridge rocks and their influence on hydrothermal circulation, *BRIDGE Newsl.*, 11, 16-18, 1996.
- Kirby, S. H., Rheology of the lithosphere, *Rev. Geophys.*, 21, 1458-1487, 1983.
- Lachenbruch, A. H., A simple mechanical model for oceanic spreading centres, *J. Geophys. Res.*, 78, 3395-3417, 1973.
- Lawn, B. R., and T. R. Wilshaw, *Fracture of Brittle Solids*, Cambridge Univ. Press, New York, 1975.
- McAllister, E., J. Cann, and S. Spencer, The evolution of crustal deformation in an oceanic extensional environment, *J. Struct. Geol.*, 17, 183-199, 1995.
- McCoss, A. M., Simple constructions for deformation in transpression/transension zones, *J. Struct. Geol.*, 8, 715-718, 1986.
- Murton, B. J., and L. M. Parson, Segmentation, volcanism and deformation of oblique spreading centres: A quantitative study of the Reykjanes Ridge, *Tectonophysics*, 222, 237-257, 1993.
- Olsen, J. E., and D. D. Pollard, The initiation and growth of en echelon veins, *J. Struct. Geol.*, 13, 585-608, 1991.
- Parsons, B., and D. P. McKenzie, mantle convection and the thermal structure of the plates, *J. Geophys. Res.*, 83, 4485-4496, 1978.
- Parsons, B., and J. G. Schlater, An analysis of the variation of ocean floor bathymetry and heat flow with age, *J. Geophys. Res.*, 82, 803-827, 1977.
- Ranalli, G., and D. C. Murphy, Rheological stratification of the lithosphere, *Tectonophysics*, 132, 281-295, 1987.
- Renshaw, C. E., and C. F. Harvey, Propagation velocity of a natural hydraulic fracture in a poroelastic medium, *J. Geophys. Res.*, 99, 21,667-21,677, 1994.
- Renshaw, C. E., and D. D. Pollard, Numerical simulation of fracture set formation: A fracture mechanics model consistent with experimental observations, *J. Geophys. Res.*, 99, 9359-9372, 1994.

- Rutter, E. H., and K. H. Brodie, Lithosphere rheology-A note of caution, *J. Struct. Geol.*, *13*, 363-367, 1991.
- Sanderson, D. J., and W. R. D. Marchini, Transpression, *J. Struct. Geol.*, *6*, 449-458, 1984.
- Segall, P., and D. D. Pollard, Nucleation and growth of strike slip faults in granite, *J. Geophys. Res.*, *88*, 555-568, 1983.
- Searle, R. C., P. R. Field, and R. B. Owens, Segmentation and a non-transform ridge offset on the Reykjanes Ridge near 58°N, *J. Geophys. Res.*, *99*, 24,159-24,172, 1994.
- Searle, R. C., and A. S. Laughton, Fine scale sonar study of tectonics and volcanism on the Reykjanes Ridge, *Oceanol. Acta*, *26*, 5-13, 1981.
- Sempere, J. C., and K. C. Macdonald, Overlapping spreading centers: Implications from crack growth simulation by the displacement discontinuity method, *Tectonics*, *5*, 161-163, 1986.
- Shaw, P. R., and J. Lin, Causes and consequences of variations in faulting style at the Mid-Atlantic Ridge, *J. Geophys. Res.*, *98*, 21,839-21,851, 1993.
- Shaw, W. J., and J. Lin, Models of ocean ridge lithospheric deformation: Dependence on crustal thickness, spreading rate, and segmentation, *J. Geophys. Res.*, *101*, 17,977-17,993, 1996.
- Simpson, C., Displacement and strain patterns from naturally occurring shear zone terminations, *J. Struct. Geol.*, *5*, 497-506, 1983.
- Talwani, M., C. C. Windisch, and M. G. Langseth, Reykjanes Ridge crest: A detailed geophysical study, *J. Geophys. Res.*, *76*, 473-517, 1971.
- Tuckwell, G. W., J. M. Bull, and D. J. Sanderson, Models of fracture orientation at oblique spreading centres, *J. Geol. Soc.*, *153*, 185-189, 1996.
- Wright, D. J., R. M. Haymon, and K. C. Macdonald, Breaking new ground: estimates of crack depth along the axial zone of the East Pacific Rise (9°N-12°54'N), *Earth Planet. Sci. Lett.*, *130*, 441-457, 1995.
- 
- J. M. Bull and D. J. Sanderson, Department of Geology, University of Southampton, Southampton Oceanography Centre, Southampton, SO14 3ZH, U.K.
- G. W. Tuckwell, Department of Earth Science, University of Liverpool, Liverpool, L69 3BX, U.K. (gwt@liv.ac.uk)

(Received March 18, 1997; revised December 4, 1997; accepted December 15, 1997.)